Nuclear motion in carbonyl sulfide induced by resonant core electron excitation

Laksman, Joakim; Céolin, Denis; Gisselbrecht, Mathieu; Ristinmaa Sörensen, Stacey

Published in:
Journal of Chemical Physics

DOI:
10.1063/1.3502116

2010

Nuclear motion in carbonyl sulfide induced by resonant core electron excitation

J. Laksman,[a] D. Céolin, M. Gisselbrecht, and S. L. Sorensen
Department of Synchrotron Radiation Research, Lund University, Lund S-221 00, Sweden

(Received 16 June 2010; accepted 24 September 2010; published online 14 October 2010)

The angular anisotropy for selected dissociation channels is measured at resonantly excited states of Σ and Π symmetries at the C and O K-shell ionization edges of carbonyl sulfide. While the kinetic energy released in the reaction is mainly independent of the excitation energy, the angular anisotropy and momentum correlation clearly show deformation of the OCS molecule in the C $1s^{-1}\pi^{*1}$ state. The discovery of a two-body fragmentation channel SO^+/C^+ with a well defined angular anisotropy indicates the rapid formation of the CSO isomeric species. © *2010 American Institute of Physics*. [doi:10.1063/1.3502116]

I. INTRODUCTION

Nuclear motion in photoexcited molecules is important for understanding basic photochemistry but is of interest from a fundamental point of view as a symmetry breaking process which can have implications for the fate of core-excited states.[1] Although electron spectroscopy can indirectly indicate a transition from linear to bent geometry the detection of one or more ionic fragments is necessary for a fixed molecular frame measurement.[2] Elegant experiments where ion- and electron-energy analysis identifies the initial and final states of the reaction provide insight into the coupling between electronic states and nuclear motion.[3] Recent studies using multicoincidence methods based on imaging spectroscopies have elucidated the details of such processes and the temporal aspects of nuclear motion are beginning to be understood.[4] Multicoincidence measurements of molecular dissociation using linearly polarized soft x-rays provide angular distributions directly in addition to kinematic information on specific dissociation channels. Core-excited states in molecules are known to be highly localized, the life time is short, and tunable synchrotron radiation allows for specific excitation to electronic states of different symmetries and localized to different sites in the molecule. Multi-ion coincidence imaging studies have illuminated geometry changes and nuclear motion in several recent synchrotron based studies and the Renner–Teller effect in CO_2 was directly confirmed by Muramatsu's study using this method.[1]

Carbonyl sulfide is linear in the ground state, but Eland showed that the dication is nonlinear.[5] For resonant excitation of the core electrons the symmetry of the transition can be used to provide an ensemble of aligned excited molecules. Erman *et al.*[6] report evidence for a bent geometry at the S $2p^{-1}\pi^{*1}$ states as determined from the double ion coincidence spectra, while at the C 1s edge the analysis was carried out on single-ion data where different atomic fragments were found to exhibit different asymmetries. Adachi[7] used the angle resolved photo-ion method to study OCS at the C $1s^{-1}\pi^{*1}$ state while Kaneyasu studied dissociation of OCS dications after S 2p ionization and found that higher-energy electronic states dissociate into CO^+/S^+ and to $O/C^+/S^+$.[8]

A recent calculation of the double ionization spectrum by Minelli *et al.*[9] finds a vertical double ionization potential at 29.4 eV ($^3\Sigma^-$ state). The threshold for the first dication fragmentation channel, CO^+/S^+, was found by Masuoka[10] at 34 eV; calculations by Ridard[11] showed that the ground state of the dication ($X\ ^2\Sigma^-$) dissociates into $CO^+(X)/S^+(^4S)$ after a 2 eV barrier. The reaction energy was calculated to be approximately 4 eV. Brites *et al.*[12] made multireference configuration interaction calculations of a number of electronic states of the dication to examine kinetic energy releases and dissociation along both O–C and C–S bonds. They found the ground electronic state to have a long lifetime before dissociation to CO^+/S^+. Furthermore, Brites discovered a possible route to the CSO^{2+} isomer whose lowest electronic state is expected to be repulsive and dissociate to C^+/OS^+ in their ground states. A recent study of OCS^{3+} produced by double Auger decay at the S 2p edge by Eland *et al.*[13] found that localization plays a strong role in the population of triply ionized states.

In the present study we measure the angular distribution of selected fragmentation channels in carbonyl sulfide at the carbon and oxygen 1s ionization edges. We measure the momenta of all ionic fragments using multicoincidence techniques. The measured kinetic energies of the fragments are used as a basis for calculating the total kinetic energy released in the reaction and the angular isotropies are extracted for each channel. We find that the C $1s^{-1}\pi^{*1}$ state shows a greater tendency to a bent geometry compared to the nonresonant case. At this core-excited state we also find evidence for production of the OS^+ fragment, which is indicative of a severely bent molecule. We analyze the triple ionized molecule by triple-ion momentum imaging. Our study shows clear evidence of both symmetry breaking and of the Renner–Teller effect at the C $1s^{-1}\pi^{*1}$ state.

[a]Electronic mail: joakim.laksman@sljus.lu.se.

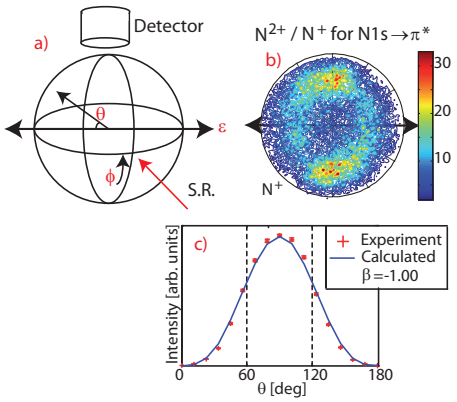

FIG. 1. (a) A schematic diagram of the geometry of the setup. (b) Two-dimensional histogram representing the detector area showing fragments from nitrogen dissociation at the N $1s^{-1}\pi^{*1}$ state. The plot shows the number of N^+ ions which arrive in coincidence with N^{2+} ions at each detector coordinate. (c) The angular distribution of all fragments from the pathway N^+/N^{2+}, from which the β-parameter has been estimated. The calculated distribution for $\beta=-1$ is shown with a solid line.

II. EXPERIMENT

A momentum imaging time-of-flight spectrometer is used for the present study. The spectrometer is mounted with the axis mutually perpendicular to the polarization vector of the x-rays and to the propagation direction of the synchrotron light [see Fig. 1(a)]. The spectrometer consists of a detector for electrons and a time-of-flight spectrometer with a two-stage acceleration with an electrostatic lens to focus ions onto an 80 mm diameter delay-line detector (Roentdek DLD80). The sample gas background pressure in the spectrometer chamber was 5×10^{-6} mbar. Lens potentials were optimized so that ions from dissociation of molecular hydrogen were imaged clearly on the detector and the energy scale was calibrated to the known H^+ fragment energy.[14] Simulations with the SIMION package[15] indicate that for the present fields ions with up to 19 eV kinetic energy are collected.

The measurements were performed at the soft x-ray undulator beamline I411 at MAX-laboratory in Lund, Sweden.[16] The photoenergy calibration was made to the published value of the OCS C $1s\rightarrow\pi^{\star}$ resonance.[7] The contribution from second-order light was found to be negligible.

The raw data for each event are transformed into a three-dimensional momentum space and subsets of the data are extracted by filtering by angular criteria, momentum or according to dissociation channel. The kinematics are extracted directly from the momentum data and the molecular anisotropy parameter, β, can be found for single ions or dissociation channels. The conventional analytical expression for the differential cross section is

$$\frac{d\sigma}{d\Omega}=\frac{\sigma}{4\pi}[1+\beta P_2(\cos\theta)], \tag{1}$$

where σ is the total cross section integrated over space and P_2 is the second-order Legendre polynomial, $P_2(x)=(3x^2-1)/2$. The geometry of our setup is shown in Fig. 1(a). Since the fragment intensity is symmetric about the polarization vector then the fragment intensity can be expressed as[17]

$$I(\theta)=\frac{\sigma}{4\pi}\int[1+\beta P_2(\cos\theta)]d\Omega, \tag{2}$$

where $d\Omega=\sin\theta d\theta d\phi$, so

$$I(\theta)=\frac{\sigma}{4\pi}\int_0^{2\pi}d\phi\int_{\theta}^{\theta+\Delta\theta}d\theta\sin\theta[1+\beta P_2(\cos\theta)], \tag{3}$$

with the solution for the case where $\delta\theta\rightarrow0$,

$$I(\theta)=\frac{\sigma}{2}\sin\theta[1+\beta P_2(\cos\theta)]. \tag{4}$$

The validity of this equation has been verified by empirical studies.

Figure 1(b) shows the spatial distribution of fragments from nitrogen dissociation at the N $1s^{-1}\pi^{*1}$ resonance. This is a projection of the 3D data onto a histogram in a polar plot. The fragment distribution is clearly perpendicular to the polarization direction indicated in the plot. Figure 1(c) shows the angular distribution of all fragments from the pathway N^+/N^{2+} plotted as a function of θ. The best fit of $I(\theta)$ corresponds to $\beta=-1.00$ in excellent agreement with the expected value.[18] Sources of systematic error include irregular detector efficiency, imperfections of the choices of spatial and temporal centers of the data, as well as the direction of the polarization vector. In order to estimate the sensitivity of the β value to these errors we translated the raw data by ±2.0 mm and 3.0 ns in time and rotated by 3°. For double coincidences θ is taken as the mean value for the two particles. This led to an error estimation $\leq\pm0.03$. The histogram bin size has no effect on the β parameter.

III. RESULTS AND DISCUSSION

A. Angular anisotropy of fragments

The symmetry of the transition is well defined and the rapid electronic decay of the core-hole ensures the validity of the axial-recoil approximation.[19] Angle-resolved photo-ion spectroscopy (ARPIS) has shown that with the exception of vibrational coupling the angular emission of fragments follows the predictions of the dipole operator for linearly polarized light.[18] Another factor which can affect the angular emission is the temporal aspect of the dissociation process. Metastable states which dissociate on the time scale of the measurement have a well defined pattern in time-of flight spectra, but more rapid stepwise dissociation can lead to smearing of the angular emission.[20]

The anisotropy of the carbonyl sulfide dissociations has been determined in a variety of studies including direct valence ionization and resonantly excited states at the sulfur and carbon edges. Masuoka[21] reported anisotropic ion distributions for the primary dissociation channels after valence ionization. Adachi *et al.*[7] measured the angular anisotropy of ions with the ARPIS method at the C $1s^{-1}\pi^{*1}$ state. Their method compares the total ion yield measured at two angles in order to extract the anisotropy. They found that at the resonance maximum β is -0.4, but it increases slightly at the low-energy side of the resonance, and attributed this to the Renner–Teller effect. Erman *et al.*[6] reported β values for

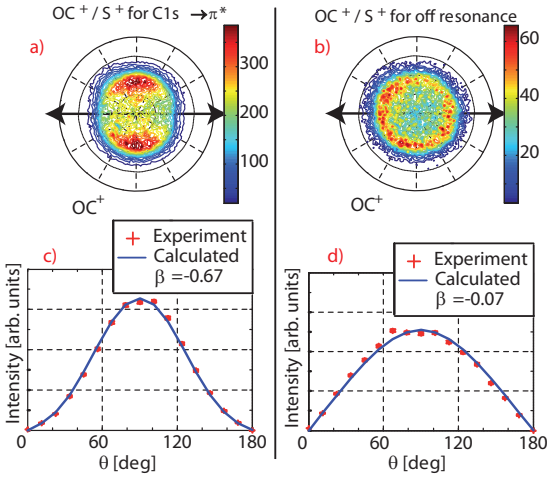

FIG. 2. Histogram of CO^+ fragments from the CO^+/S^+ dissociation channel for resonant and nonresonant cases. (a) Distribution of fragments at C $1s^{-1}\pi^{*1}$ (288.08 eV). (b) Distribution of fragments measured at 285 eV. The direction of the polarization vector is shown. The distribution of fragments is plotted as a function of the angle θ (see Fig. 1) after integration of Eq. (3) for (c) C $1s^{-1}\pi^{*1}$ and (d) off resonance.

mass-selected fragment ions in a study covering the sulfur 2p and carbon 1s edges. The fragment asymmetries at the S $2p^{-1}\pi^{*1}$ states indicate a bent geometry.

Our results compare favorably with earlier measurements but some notable differences exist. Our measured CO^+ momentum plot contains two separate distributions with very different momenta. The low-momentum ions arise from dissociation of OCS^+, while dication fragmentation leads to higher-energy CO^+ ions. The anisotropies differ as well; we find β is -0.14 ± 0.03 and -0.68 ± 0.03 for the two cases. Erman's study reports a CO^+ β value of -0.6, clearly only corresponding to the higher momentum fragment. We have not found any other similar energy-dependent fragment anisotropies.

Resonant excitation primarily influences the angular distribution of fragments. In Fig. 2 the CO^+/S^+ dissociation channel for the C $1s\rightarrow\pi^*$ resonance is compared to the off resonance case. We plot the distribution of CO^+ ions from this channel on the detector (thus ignoring the momentum along the spectrometer axis) producing a polar plot equivalent to the velocity map image. The polarization vector of the light is indicated in the polar plot. The distribution clearly shows an alignment perpendicular to the polarization direction for the resonant excitation with a well defined radial distribution while the angular distribution off resonance is more or less isotropic. In subplots (c) and (d) we present the fully integrated angular distributions derived from the 3D data sets using Eq. (3). The calculated distribution which best fits the experimental data is shown as a solid line. The β value of -0.67 is roughly equal to the expected value for a perpendicular transition for a triatomic molecule. The nonresonant distribution is close to isotropic and represents the sum of several ionization channels with different symmetries.

In Table I we present the molecular β values for two-body dissociation channels near the C 1s and O 1s ionization edges. We have measured spectra both above and below the resonance regions but for all off resonance spectra the results are similar. The average anisotropy for the two fragments is calculated after filtering the data for the selected dissociation channel and the integration is performed as described above. For the C $1s\rightarrow\pi^*$ resonance the anisotropies for the CO^+/S^+ and O^+/CS^+ channels are similar but not identical. Adachi reported a β value of -0.4 for the ARPIS measurement of all ions.[7] We can reproduce this value when we analyze the distribution of all ions irrespective of coincidence degree but excluding zero-energy ions.

TABLE I. Angular asymmetry parameters for dissociation channels at the C 1s and O 1s ionization edges. The estimated error in these values is $\pm\leq0.03$.

Pathway	O^+/CS^+	S^+/CO^+
270 eV	0.14	−0.07
C $1s\rightarrow\pi^*(000)$	−0.75	−0.67
C $1s\rightarrow\sigma^*$	+0.10	−0.11
O $1s\rightarrow\pi^*$	−0.70	−0.57
O $1s\rightarrow\sigma^*$	0.41	0.31

The anisotropy for the O^+/CS^+ channel is nearly always greater than the value for the S^+/CO^+ channel, independent of the photon energy. We believe that this is significant despite it being a weak effect. We exclude instrumental effects where anisotropy depends on the flight-time, since both fragments from one pair have the same anisotropy. The lower β for S^+/CO^+ suggests that the dicationic state leading to this dissociation channel has significant bending vibrational excitation. Another contributing factor is the life time; a long life time with respect to the rotational period decreases the measured β. This is supported by Brites'[12] finding of a long-lived dication ground state which dissociates into the S^+/CO^+ pair.

For all of the photon energies we have measured the intensity of the S^+/CO^+ is always 10–15 times greater than for the O^+/CS^+ channel. Calculated potential-energy surfaces show that the O^+/CS^+ channel is at the lowest energy. Brites *et al.*[12] calculation of the dication orbitals shows an increasing electron density in the C–O bonding π orbital thus strengthening the C–O bond. The C–S orbital, on the other hand, loses charge, and the C–S bond length is increased.

The kinetic energy released in the two-body dissociation channels reflects the potential surface in the dication which leads to dissociation. We have studied the CO^+/S^+ and O^+/CS^+ reactions which show only small differences in the total kinetic energy for on and off resonance, and excitations at the C 1s and O 1s edges. In fact, the kinetic energy released (KER) is consistent with Masuoka's[22] study in the inner-valence region where they find a KER 3–8 eV for the CO^+/S^+ channel. This implies that the same dissociative states are populated and that those states are already accessible at 45 eV photon energy.

A similar analysis can be carried out on three-body dissociation channels where two atomic ions are produced. For the C $1s\rightarrow\pi^*$ state we consistently find that the terminal fragments (O and S) have negative anisotropy parameters while the C fragment β is positive. This clearly indicates and overall alignment perpendicular to the polarization vector and a bent geometry. For all photon energies, carbon and

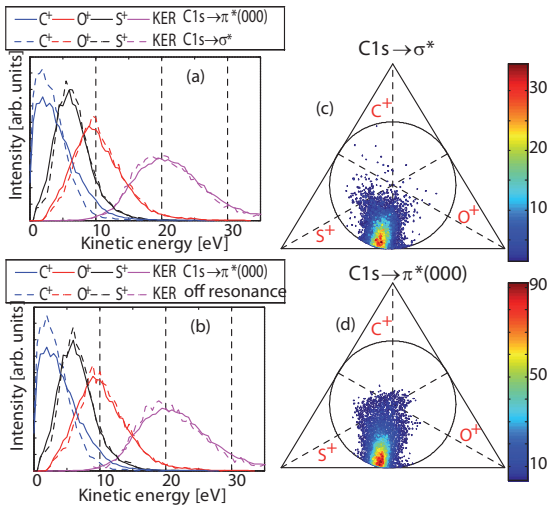

FIG. 3. The KER distribution of each fragment and the total kinetic energy. (a) C $1s\rightarrow\pi^*$ compared to C $1s\rightarrow\sigma^*$ (b) C $1s\rightarrow\pi^*$ compared to off resonance. The ratios of fragment energies presented in a Dalitz plot (c) C $1s\rightarrow\sigma^*$ and (d) C $1s\rightarrow\pi^*$.

oxygen fragments from $C^+/O/S^+$ have smaller anisotropy than from $C^+/O^+/S$ and $C/O^+/S^+$. This makes sense if the former is a sequential process where the intermediate CO^+ fragment rotates before dissociation. The latter two have a sharper anisotropy indicating rapid dissociation via Coulomb explosion. The same phenomenon is visible in the inner-valence region.[10] Our KER values for the $C/O^+/S^+$ and $C^+/O/S^+$ channels are very similar to Masuoka's[22] measurements at 100 eV.

B. Dissociation of the triply ionized molecule

The anisotropy parameters for the terminal fragments are very similar to the dication fragmentation suggesting a concerted explosion. We also find that $\beta(C^+)$ is generally of opposite sign than the other fragment anisotropy parameters. $\beta(C^+)$ at the C $1s\rightarrow\pi^*(000)$ resonance is typical of a parallel transition ($\sim$0.69) and is explained by the nuclear dynamics in the C $1s^{-1}\pi^{*1}$ state. The molecule is not only bent in the final dissociative state, but the bending preferentially occurs in a specific direction so that the dipole moment has a tendency to align with the polarization. This is evidence that the core-excitation process cannot be separated from the dissociation dynamics.[23]

Lavollée *et al.*[24] find that the KER primarily reflects the Coulomb repulsion between fragments after ionization and is independent of the electronic state. In Fig. 3 we present individual fragment KER and the total KER at the C $1s\rightarrow\pi^*(000)$ resonance at 288.2 eV, which is compared with C $1s\rightarrow\sigma^*$ resonance at 311.5 eV and to the off C1s resonance case at 286 eV. Our measured total KER distributions exhibit no significant changes as a function of photon energy in accord with Lavollée's finding. At the C $1s\rightarrow\pi^*$ resonance there is a redistribution of kinetic energy among the fragments. The terminal ions O^+ and S^+ have lower kinetic energies while C^+ has a significant shift to higher-energy at resonance. For the two S $2p\rightarrow\pi^*$ spin-orbit split states (not presented here) we find similar energies while for all other photon energies the distributions are nearly identical to those from C $1s\rightarrow\sigma^*$. This implies significant bending in the C $1s^{-1}\pi^*$ and S $2p^{-1}\pi^*$ states.

C. Fragment correlation

Coincidence techniques provide another means of analysis since we also measure the vector correlation between fragments. The normalized coordinates ϵ_i derived from the squared momenta are defined as

$$\epsilon_i = \frac{|\vec{p}_i|^2}{\Sigma_{i=1}^{3}|\vec{p}_i|^2}, \tag{5}$$

and $\vec{p}_i$ is the momentum vector of fragment $i\in\{1,2,3\}$. The kinematic constraint, $\Sigma_i\epsilon_i\equiv 1$, requires all points to lie on a plane. Conservation of linear momentum $\Sigma_i\vec{p}_i\equiv\vec{0}$, introduces the additional constraint that all points must lie within the unit-circle. Introduction of Cartesian coordinates $x_D=(\epsilon_2-\epsilon_3)/\sqrt{3}$ and $y_D=\epsilon_1-1/3$ allows data to be presented in a 2D Dalitz plot from which the vector correlation between fragments can be deduced.[25,26]

Dalitz plots for C $1s\rightarrow\pi^*$ and C $1s\rightarrow\sigma^*$ resonances are shown in Figs. 3(c) and 3(d). For interpretation of this KER-correlation plot we project the data on to each of the three Dalitz axes. The case where particle i has zero momentum corresponds to the point where the tangent of the circle is perpendicular to the ϵ_i-axis. The opposite point represents the maximum value $\epsilon_i=2/3$. At the center coordinate all fragments have equal momenta. For both photon energies the maximum density is at low ϵ_{C^+} values which makes sense for the central atom in a triatomic molecule. However, at the C $1s\rightarrow\pi^*$ resonance, there are a significant number of events lying at higher ϵ_{C^+} values so at resonance C^+ gains a larger fraction of the KER.

The shape of the regression distribution in the Dalitz plot is closely connected to the time scale of the dissociation. By analyzing the distributions we can distinguish between sequential and concerted processes.[4] For a sequential dissociation in the ABC molecule ($ABC\rightarrow A+BC\rightarrow A+B+C$) the diatomic fragment, BC, has time to rotate between the first and second bond breaks. In this case we expect B and C to be anticorrelated, while A, which receives a nearly constant fraction of the total KER, should be uncorrelated with the other fragments. In Figs. 3(c) and 3(d) none of the particles show evidence of anticorrelation. This confirms the hypothesis of a concerted process where all particles are in the Coulomb region during breakup. We arrived at the same conclusion earlier regarding the O^+ and S^+ fragments based on their similar anisotropies.

The fact that $\epsilon_{S^+}>\epsilon_{O^+}$ implies that S^+ receives slightly more momentum than O^+. The time-of-flight correlation plots from the triple coincidences follow the same pattern since the slope $\Delta T_{S^+}/\Delta T_{O^+}\approx -1.2$ because the time deviation is proportional to the momentum deviation.[27] We also studied Dalitz plots for the dicationic three-body breakups and found that both $C/O^+/S^+$ and $C^+/O^+/S$ display uncorrelated patterns similar to those in Figs. 3(c) and 3(d), thus confirming the concerted dissociation. $C^+/O/S^+$, on the other hand, has a sharp regression perpendicular to the S^+ axis, thus C^+

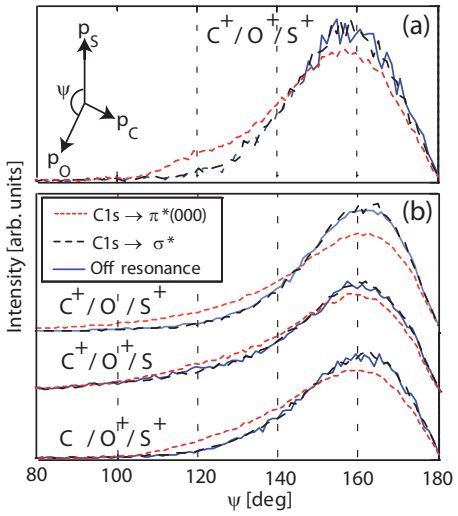

FIG. 4. Angular correlations between fragments from complete dissociation to atomic fragments. Each plot contains the data for excitation to the C $1s^{-1}\pi^{1*}$ state, the C $1s^{-1}\sigma^{1*}$ state and the off resonance measurement. (a) Histogram as a function of angle ψ for the triple ionization events. (b) Histogram as a function of angle ψ for the three-body double ionization events. ψ is defined as the angle between the vectors p_O and p_S.

and O are highly anticorrelated which confirms primary ejection of the sulfur cation followed by dissociation.

The higher C^+ energy seen in the Dalitz plots of the C $1s^{-1}\pi^*$ state also implies that the terminal atoms approach each other. To this end we plot a histogram of the angle ψ between the momentum vector of O^+ and S^+ in Fig. 4(a). The angle is shown in the inset in Fig. 4. The plot shows a smaller angle for the C $1s^{-1}\pi^*$ state.

The correlation between angles also provides information on bending so we include triple dissociation in this analysis. In Fig. 4(b) we plot angular correlations for these dissociation channels. The information about the neutral particle was extracted by conservation of momentum. Again we find similar distributions for all excitation energies except for the C $1s^{-1}\pi^{*1}$ state where the molecule is bent.

The bent and the linear components of the Renner–Teller states can be resolved separately by taking the alignment of the components into account.[1] For $\Sigma-\Pi$ dipole transitions the bending mode of the linear state defines a plane perpendicular to that of the polarization vector ϵ, while for the bent state with in-plane π orbitals the molecule lies in the plane defined by ϵ and the photon propagation direction. Coincidence events where the center fragment, C^+, has a momentum vector within a solid angle $\pm 4°$ about ϵ arise from the A_1 component while for the linear B_1 component, the cross-product for the terminal fragment's momentum vector is within the same solid angle. The distributions are independent of the chosen solid angle. Intensity normalized histograms of the distribution of angle between O^+ and S^+ fragments with respect to C for the two Renner–Teller split components are compared in Fig. 5. The diagram shows that the angles are similar for both states, but the A_1 component has a smaller average angle. This is evidence that static Renner–Teller splitting is the impetus for the bending of the molecule in the C $1s^{-1}\pi^{*1}$ state. Kukk *et al.*[28] found in resonant Auger electron spectra from carbon dioxide that the A_1

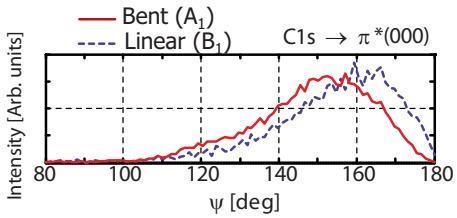

FIG. 5. A histogram of the intensity as a function of bond angle (Ψ) for the two Renner–Teller components at the C $1s \rightarrow \pi^*$ state. The events corresponding to the bent geometry (A_1) and the linear geometry (B_1) are compared.

state is populated mainly at the left edge of the C $1s \rightarrow \pi^*$ resonance. We investigated the population of the A_1 and B_1 states at different photon energies within the resonance but found no significant variation.

The S $2p \rightarrow \pi^*$ state exhibits the same tendency to a bent geometry as we found at the C $1s \rightarrow \pi^*$ resonance for both spin-orbit components. The states at the O 1s edge show no resonance dependence of the angle (see Fig. 6), thus no Renner–Teller effect is visible. This is in contrast with the CO_2 study of Muramatsu who also observed the bent state at the O $1s \rightarrow 2\pi_u$ resonance.[1]

D. Isomerization

A consequence of the Renner–Teller effect is the tendency for isomerization to the CSO species. Brites *et al.*[12] calculated potential surfaces in the dication and found the energetic barrier from the linear to bent geometry is about 4 eV. Their calculations indicate that in addition to the dissociation channels discussed so far an isotopic form is energetically possible. The isotopic species requires a deformation to an angle of about 150°, which leads to a breaking of the CO bond, and the forming of a new bond between O and S. We have found a weak population of this channel where the finger print is coincident detection of C^+ and OS^+ ions. The signal is detectable at all energies in our study, but at the C $1s \rightarrow \pi^*$ and the S $2p \rightarrow \pi^*$ state this channel has a significantly higher branching ratio.

In Fig. 7(a) we plot the total KER for the C^+/OS^+ dissociation channel. The distribution peaks at between 4 and 5 eV, which despite the poor statistics, is in reasonable agreement with Brites' predicted value.[12] The angular distribution of fragments and a fit to the anisotropy are shown in Fig. 7(b). The estimated positive value ($\beta \approx 0.39$) is far from totally anisotropic, but is still in qualitative agreement with a parallel transition, suggesting that the excitation induces the bending. Auger decay then populates electronic states in the dication and dissociation is prompt.

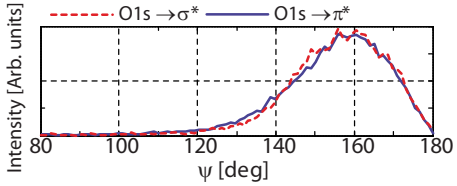

FIG. 6. Comparison of angular correlations from the three-body breakup of OCS^{3+} for O $1s^{-1}\pi^{*1}$ and O $1s^{-1}\sigma^{*1}$ states.

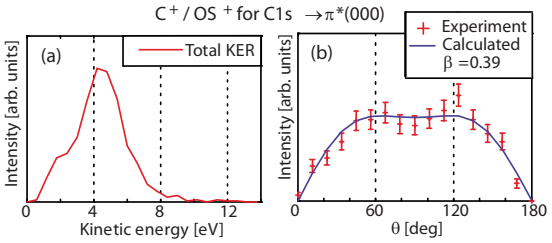

FIG. 7. The C^+/OS^+ channel was found at the C $1s-\pi^*$ state. This channel arises as a consequence of isomerization of the dication. (a) The KER distribution. (b) The angular distribution of fragments and a fit to the β parameter. The positive anisotropy implies that the bending motion cannot be separated from the core-excitation.

The selection of this specific channel gives us important information not only on the final dissociation state, but it tells us that the nuclear motion in the core-excited state and the photon absorption process cannot be regarded as separate for this particular case. Indeed, at the time of the excitation, photoabsorption certainly triggers the nuclear motion. The bending mode can be excited and the corresponding transition dipole moment is in-plane and perpendicular to the initial $C_{\infty v}$ axis. By selecting the C^+/OS^+ fragment, we only monitor molecules undergoing a bending motion, with a transition dipole moment aligned with the polarization axis. The subsequent dissociation retains the memory of this alignment, which is reflected in the intensity distribution of the ejected fragments, parallel to the polarization vector, $\vec{\epsilon}$. From the triple-coincidence channel, we have found that the bending motion that causes isomerization is enhanced in the C $1s^{-1}\pi^{*1}$ and S $2p^{-1}\pi^{*1}$ state.

IV. CONCLUSION

Analysis of the kinematics of fragmentation of the OCS molecule at several ionization energies has provided a clear picture of nuclear motion during the core-hole life time. We find at the C $1s\rightarrow\pi^*$ resonant excitation that we induce a bending mode in the molecule. Further we find that this bending mode is enhanced in the Renner–Teller split A_1 state. Analysis of the three-body dissociation channels indicates that concerted dissociation is the primary mechanism for fragmentation. Our study identifies the isomeric form CSO via measurement of the C^+/OS^+ ion pair, which is found to have a unique anisotropy. The experimental method is also shown to be a tool for revealing important information on the temporal sequence of three-body dissociation processes.

ACKNOWLEDGMENTS

We gratefully acknowledge assistance from the MAX-laboratory staff, in particular to Maxim Tchaplyguine. Funding for this work was granted from the Knut and Alice Wallenberg foundation and the Swedish Research Council (VR).

[1] Y. Muramatsu, K. Ueda, N. Saito, H. Chiba, M. Lavolée, A. Czasch, T. Weber, O. Jagutzki, H. Schmidt-Böcking, R. Moshammer, U. Becker, K. Kubozuka, and I. Koyano, Phys. Rev. Lett. **88**, 133002 (2002).
[2] J. H. D. Eland and E. J. Duerr, Chem. Phys. **229**, 1 (1998).
[3] R. Dörner, H. Schmidt-Böcking, V. Mergel, T. Weber, L. Spielberger, O. Jagutzki, A. Knapp, and H. P. Bräuning, in *Many-Particle Quantum Dynamics in Atomic and Molecular Fragmentation*, edited by V. P. Shevelko and J. Ullrich, (Springer-Verlag, Berlin, 2002).
[4] K. Ueda and J. H. D. Eland, J. Phys. B **38**, S839 (2005).
[5] J. H. D. Eland, Mol. Phys. **61**, 725 (1987).
[6] P. Erman, A. Karawajczyk, E. Rachlew, M. Stankiewicz, and K. Yoshiki-Franzén, Phys. Rev. A **56**, 2705 (1997).
[7] J. Adachi, N. Kosugi, E. Shigemasa, and A. Yagishita, J. Chem. Phys. **107**, 4919 (1997).
[8] T. Kaneyasu, M. Ito, Y. Hikosaka, and E. Shigemasa, J. Korean Phys. Soc. **54**, 371 (2009).
[9] D. Minelli, F. Tarantelli, A. Sgamellotti, and L. S. Cederbaum, J. Chem. Phys. **107**, 6070 (1997).
[10] T. Masuoka, J. Chem. Phys. **98**, 6989 (1993).
[11] J. Ridard, B. Levy, and P. Millie, Chem. Phys. **122**, 403 (1988).
[12] V. Brites, J. H. D. Eland, and M. Hochlaf, Chem. Phys. **346**, 23 (2008).
[13] J. H. D. Eland, M. Hochlaf, P. Linusson, E. Andersson, L. Hedin, and R. Feifel, J. Chem. Phys. **132**, 014311 (2010).
[14] G. Dujardin, M. J. Besnard, L. Hellner, and Y. Malinovitch, Phys. Rev. A **35**, 5012 (1987).
[15] D. A. Dahl, *Simion 3D version 7.0 User's Manual* (Idaho National Engineering and Environmental Laboratory, 2000).
[16] M. Bässler, A. Ausmees, M. Jurvansuu, R. Feifel, J. O. Forsell, P. de Tarso Fonseca, A. Kivimäki, S. Sundin, S. L. Sorensen, R. Nyholm, O. Björneholm, S. Aksela, and S. Svensson, Nucl. Instrum. Methods Phys. Res. A **469**, 382 (2001).
[17] A. I. Chichinin, T. S. Einfeld, K. H. Gericke, and C. Maul, in *Imaging in Molecular Dynamics*, edited by B. Whitaker (Cambridge University Press, New York, 2003), pp. 153–155.
[18] J. Adachi, N. Kosugi, and A. Yagashita, J. Phys. B **38**, R127 (2005).
[19] R. N. Zare, Mol. Photochem. **4**, 1 (1972).
[20] T. Osipov, C. L. Cocke, M. H. Prior, A. Landers, Th. Weber, O. Jagutzki, L. Schmidt, H. Schmidt-Böcking, and R. Dörner, Phys. Rev. Lett. **90**, 233002 (2003).
[21] T. Masuoka and I. Koyano, J. Chem. Phys. **95**, 909 (1991).
[22] T. Masuoka, I. Koyano, and N. Saito, J. Chem. Phys. **97**, 2392 (1992).
[23] J. Laksman, D. Céolin, M. Gisselbrecht, S. E. Canton, and S. L. Sorensen, J. Chem. Phys. **131**, 244305 (2009).
[24] M. Lavollée (private communication).
[25] R. H. Dalitz, Philos. Mag. **44**, 1068 (1953).
[26] C. Maul and K. H. Gericke, J. Phys. Chem. A **104**, 2531 (2000).
[27] M. Simon, T. Lebrun, R. Martins, G. G. B. de Souza, M. Lavollée, and P. Morin, J. Phys. Chem. **97**, 5228 (1993).
[28] E. Kukk, J. D. Bozek, and N. Berrah, Phys. Rev. A **62**, 032708 (2000).